Dryden Research Lecture

Atmospheric Turbulence

JOHN C. HOUBOLT
Aeronautical Research Associates of Princeton Inc., Princeton, N.J.

Atmospheric turbulence and its influence on the flight and design of aircraft is reviewed. Coverage includes accidents and costs incurred as a result of turbulence, the mechanisms of turbulence measurements that are made, aircraft response and design procedures due to turbulence encounter, and loads alleviation devices. Basic research notions associated with the interpretation of turbulence data, some of which are controversial, and areas of weakness, are also discussed.

Introduction

IN 1942 Dr. H. L. Dryden wrote a paper entitled "A Review of the Statistical Theory of Turbulence," a paper which became a classic![1] Now, thirty years later, I have been asked to write this year's research lecture in his name. Remembering his belief in the value of basic research, his individual contributions, his talents and leadership abilities, and his ability to talk or lecture so beautifully, I consider it a great honor to have been chosen for this task.

My subject matter is also turbulence, but with particular reference to atmospheric turbulence. I would like to bring out certain basic research efforts that have been conducted in this field and, in addition, indicate engineering problems and applications as involved in the flight of aircraft. It must be recognized that atmospheric turbulence has had a profound influence on the design and operation of aircraft, and so a combined consideration of research effort and application seems fitting.

Dr. Dryden's introduction to his review paper started with the paragraph: "The irregular random motion of small fluid masses to which the name turbulence is given is of such complexity that there can be no hope of a theory which will describe in detail the velocity and pressure fields at every instant. Existing theories may be classified as either empirical or statistical." The coverage herein adheres to this classification, and deals mainly with the statistical theories and the statistical and empirical observations relative to atmospheric turbulence modeling and aircraft response to this environment.

Problems Created by Atmospheric Turbulence

General

Very few perhaps recall that Technical Report 1 (Ref. 2) of NACA dealt with aircraft behavior in rough air. Also, many of the individuals who work in aerospace activity probably feel that

John C. Houbolt

Dr. Houbolt has a diversified background of experience in the fields of civil, aeronautical, and space flight engineering. He joined Aeronautical Research Associates of Princeton Inc. in 1963 after 21 years with the NASA at Langley Research Center. There he was involved with research on aircraft structures, later became Associate Chief of the Dynamic Loads Division pursuing research problems in vibration and flutter, gust loads, structural dynamics, water impact and landing loads, and acoustics, and later became Chief of the Theoretical Mechanics Division, engaged in research on special problems of space flight. He is presently Senior Vice President and Senior Consultant of A.R.A.P.

He is internationally recognized in his fields and has written over eighty technical reports, many of which are of fundamental lasting significance. In 1963, he received NASA's Exceptional Scientific Achievement Award for his development of the Lunar Orbit Rendezvous plan, the central element in the United States manned lunar exploration program. Since joining A.R.A.P., Dr. Houbolt has been a consultant to the Air Force Office of Scientific Research, the Aerospace Research Laboratories of the Air Force, NASA, General Electric Company, Grumman Aerospace, Martin Marietta Corporation, RCA Corporation, McDonnell-Douglas Corporation, and the Naval Air Engineering Center. His recent work has involved developments in the application of power spectral techniques to aeronautical problems such as gust encounter, structural response of re-entry vehicles to boundary layer noise, analysis of the intensity and spectral content of turbulent boundary layers and wakes, nonsteady aerodynamics, and with special studies such as the development of Surface Effects Vehicles.

Dr. Houbolt received his B.S. (C.E.) and M.S. (C.E.) from the University of Illinois and his Ph.D. in Technical Science from ETH (Swiss Federal Institute of Technology). He is associated with the Air Force's Scientific Advisory Board. He is a Fellow of the American Institute of Aeronautics and Astronautics and was its Vice President—Technical, and served as an associate editor of the *Journal of Spacecraft and Rockets*. He is a member of Tau Beta Pi and Sigma Xi, Chi Epsilon, and Phi Kappa Phi. Dr. Houbolt was a recipient of the Rockefeller Public Service Award, received the first Structures and Materials Award presented by the AIAA in 1968, the University of Illinois Illini Achievement Award in 1970, and the AIAA Dryden Research Lecture Award in 1972.

Presented as Paper 72-219 at the AIAA 10th Aerospace Sciences Meeting, San Diego, Calif., January 17–19, 1972; submitted March 7, 1972; revision received December 11, 1972. The author expresses sincere appreciation for the honor of having been chosen the recipient of the Dryden Research Lecture Award for the year 1972.

Index categories: Aircraft Gust Loading and Wind Shear; Aircraft Structural Design (Including Loads).

the "old" problem of flight of aircraft through rough air does not have continuing widespread significance. Upon examination, however, one finds the breadth of the problems created somewhat surprising. In general terms, severe turbulence is of concern because of the control "upset" problem and because of its influence on the static design strength of the aircraft, while moderate turbulence is of concern because it leads to problems in achieving precise flight and is a major source of fatigue damage to the aircraft structure. Some of the more specific problems created by turbulence are identified in Ref. 3. The points of this report, although written in 1966, are valid even today; a review of some of these points thus serves well to illuminate the extent and nature of the flight problems that are created by atmospheric turbulence. In 1964 alone, there were 8500 pilot reports of turbulence encounter of the unanticipated clear air variety. Of these, 670 were judged to be in the moderate, severe, and extreme categories.

Generally, turbulence encounter affects all aviation activities, including defense and civil operation, in the following ways: a) mission cancellation and diversion around turbulence; b) increased aircraft inspection; c) temporary loss of aircraft control; resultant injury to passengers and crew requiring compensation or medical treatment; d) shortening of operational time due to fatigue; e) need for special aircrew training; f) shortage of airspace due to increased number of "baby jets."

Certain aspects unique to civil and military operation are also present. In 1964, for civil aircraft alone, it is estimated that due to injury, diversions, training, information and inspection, a total expense of $18,000,000 was involved due to turbulence encounter. This figure does not include loss of the use of grounded aircraft, loss of time due to injuries, or expenses of settling claims. Also the increase in number of general aviation jets, operating in the 20,000–40,000-ft environment where restrictions vertically and horizontally may be imposed at times due to turbulence, results in increased economic concern to operators.

Military aircraft have also experienced numerous accidents and incidents because of turbulence. Additional difficulties presented to military operations include: a) hazard in air-to-air refueling, b) reduced available airspace for conducting simulated missions, and c) degradation of reconnaissance sensor and bombing accuracies.

The cost of turbulence to DOD operations is difficult to evaluate, but estimates for the 3-yr 1963–1965 period due to aircraft lost and damaged are placed around $30,000,000. Costs of special inspections, minor repairs, minor injuries, and for special training are not known. In addition, value cannot be placed on loss of pilots or on the effect on actual combat missions due to lack of advance information on the location of clear air turbulence.

A further indication of the influence of turbulence on aircraft flight can be given in terms of limit load exceedances. Statistical flight data for commercial aircraft indicate that the number of limit load exceedances per mile of flight is on the order of 10^{-6} A fleet of one thousand aircraft, each traveling an average of one million miles per year, would thus be expected to encounter 1000 limit load exceedances per year.

Jet Upset

The problem of the control of the aircraft in turbulence has been with us since the first airplane. This problem was highlighted and publicized by the popular phrase "jet upset" in the 1963–1964 time period due to a number of incidences involving loss of control and even crashes of jet aircraft. The following factors appeared common to a number of the cases: 1) control was lost in turbulent air conditions, most always in a climb condition; 2) unusually high pitch attitudes preceded a dive at high speed; 3) the dives involved speeds in excess of 460 K IAS at steep nose-down attitudes; 4) successful recoveries were made only after visual outside reference was established; 5) recovery efforts were complicated by high elevator forces and stalling of the stabilizer drive actuator. Lower elevator effectiveness of jets compared to propeller-driven aircraft, a sudden downdraft following an updraft, pilot's misinterpretation of motion cues, slow moving stabilizers and stalling of the stabilizer drive screw, all appeared as contributing causes to the problem. Fortunately, through the combined efforts of airline personnel, research personnel and industry,[4–6] particularly with respect to training and changes in operational procedure, the crisis appears to be overcome at the moment.

Table 1 Some accidents due to turbulence; 1948–1963

Probable cause	No. of aircraft
Crashed after out-of-control without disintegration in flight	3
In-flight failure after out-of-control	7
Overstressing in severe turbulence	3
Gust loads in excess of design strength	3
Failure of weakened structure in severe turbulence	3
Aircraft disappeared in severe turbulence, no further details available	3
	22

Accidents Caused by Severe Turbulence

Table 1 presents a listing of some of the kinds of accidents that have been caused by severe turbulence during the 1948–1963 time period,[7] prior to the encounter of the jet upset problem. One of the most difficult aspects about analyzing an accident due to turbulence is that of establishing whether the loads due to turbulence were sufficiently large to break the structure, or whether failure occurred because of excessive loads generated by the pilot in attempting to regain control of the aircraft. The consensus appears to be that the main hazard is loss of control followed by structural breakup during recovery attempts.

Some interesting additional results were found in an analysis of accidents due to turbulence for swept-wing commercial aircraft of U.S. carriers alone in the 1960–1963 time period. Twenty accidents, ranging in severity from injuries to crew members to total destruction of an aircraft were recorded. Nearly all the air carriers were involved. There was no specific concentration geographically; the distribution of accidents was rather random over the United States and several occurred outside the U.S. borders. The accidents occurred at all altitudes with a range of 4000–39,000 ft. In many cases, there was no advanced warning; in some, clouds were in the area. Loads ranged from $-3g$ to $+4.5g$. One aircraft landed with wrinkled skin, another lost an engine.

Sources of Turbulence

This section reviews the various atmospheric phenomena that create turbulence. The primary cause of turbulence is of course the sun as it affects the air flow over our Earth; the rotation of the Earth aggravates these flows, largely through a Coriolis force effect. In a broad sense, turbulence may be classified into two types, that due to wind shear, and that due to convection, even though shear is a basic ingredient in convection phenomena.

Turbulence due to Wind Shear

Figure 1 depicts four types of turbulence generation due to wind shear. The first, Fig. 1a, is that of a frictional shear caused by obstructions or irregularities on the ground, often called terrain mixing. The second, Fig. 1b, is due to free wind shear and is governed largely by the vertical gradient of the wind profile; this kind of turbulence can appear at various altitudes, especially at jet stream altitudes when the wind gradients are severe. Figure 1c depicts the mechanically-induced or mountain shear type of turbulence. Wind flow over mountains often exhibits four characteristics: turbulence on the immediate lee side, a stratified gravity wave pattern, extending for great distances on the lee side, shear-induced "rotors" under the crests of the gravity waves, and lenticularlike clouds at altitude in the wave crests. The lee

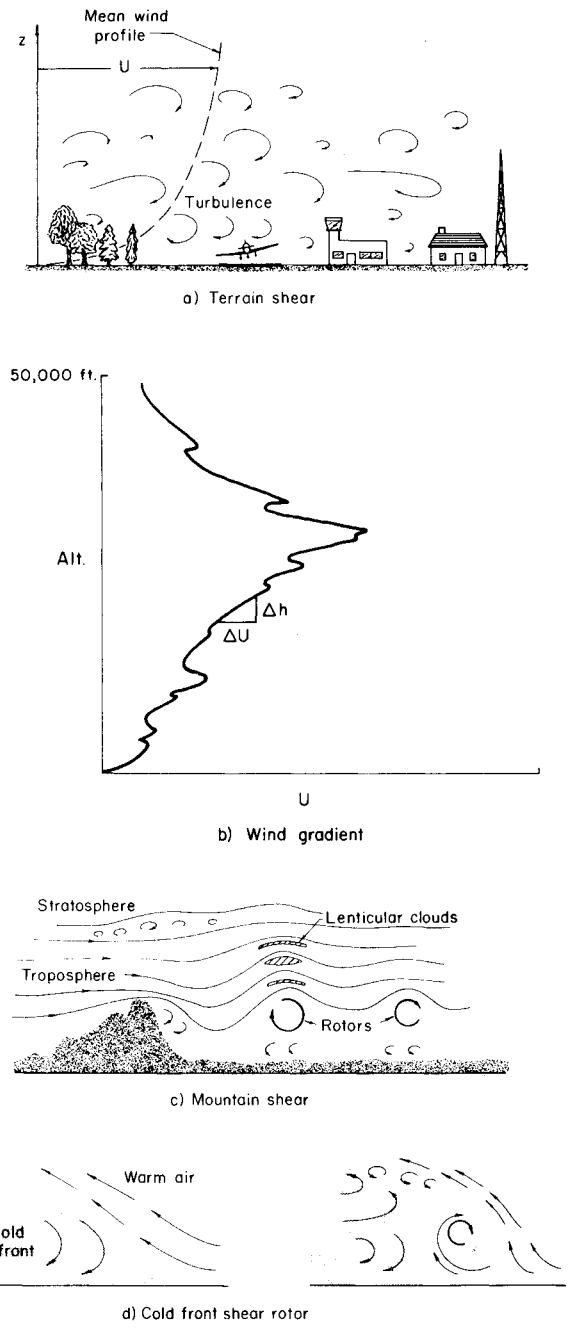

Fig. 1 Turbulence produced by shear.

side turbulence and turbulence associated with the rotors can be especially severe. The waves that are formed are quite interesting; they can be quite strong and yet actually be turbulence free, and wavelengths are often in the range of 5–10 miles. The frequency of these waves is given by the equation

$$\omega = [(g/T_0)\partial T/\partial z]^{1/2}$$

in meteorology, sometimes referred to as the Brunt-Vaiasala frequency; T is the potential temperature and T_0 is ambient absolute temperature.

Clear air turbulence is generally defined as any turbulence not in or near clouds or visible convective phenomena. Thus, Figs. 1a, b, and c depict some of the more common sources of clear air turbulence generation. Figure 1d illustrates a theory that has been advanced relative to the generation by shear of severe "rotors" by a moving cold front; this type of formation is believed to be the cause of the crash of a BAC-111 airplane in Nebraska in August 1966.

Turbulence by Convection

Figure 2 depicts the generation of turbulence by convection. The most common is that of the Benard cell type, Fig. 2a, which can be demonstrated vividly by placing a shallow pan of water over a uniform heat source. Reference 8 describes an investigation of clear-air convective patterns. Essentially, two types of convective patterns were observed. One was small thermal cells which were 0.5–1.5 miles in diameter, 600–1600 ft in height. The other type was composed of Benard-type cells, involving a number of smaller Benard cells surrounding a larger central "downdraft" cell having diameters of 3–6 miles and heights of 0.6–1.2 miles.

When a prevailing steady wind exists, the Benard cells are noted to shift into a fairly regularly spaced row cell structure, as shown in Fig. 2b. In spite of the fact that many measurements of turbulence have been made using an airplane as a probe, there do not seem to be any measurements made on the row cell-type pattern. Measurement along a path normal to the line of cells is considered worthwhile, and could be expected to yield a distinct wave pattern consisting of turbulence velocities superimposed on a sinusoidal-type wave. It may be of interest to mention that much has been learned about convective patterns by observing the soaring of herring gulls. In light winds with cool air over a warm ocean, birds are observed to soar in circular patterns delineated the columnar or Benard cell thermals. When the winds are moderate, soaring takes place along the vertical sheets which seemingly extend indefinitely up and down parallel to the winds, as depicted in Fig. 2b.

When no clouds result, the Benard cell and row cell formations are considered sources of clear air turbulence, as in the case of clear air wind shear.

The most common visual sign of convection is the "fair weather" cumulus cloud, which is formed by the vertical currents carrying moist air upward to its condensation point. Larger forms of visible convection, usually exhibiting greater turbulence severity, are shown in Figs. 2c–e.

The thunderstorm, Fig. 2c, is composed of extremely strong updraft and downdraft, and cells appear to be 0.5–1 mile in

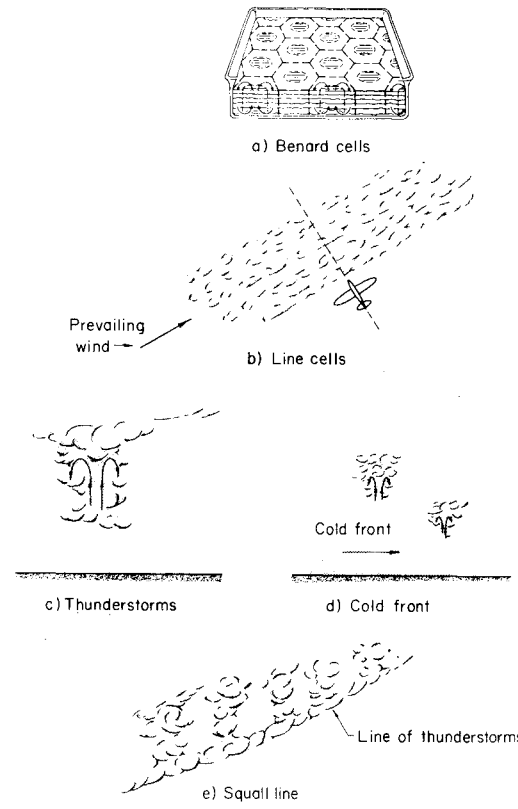

Fig. 2 Turbulence by convection.

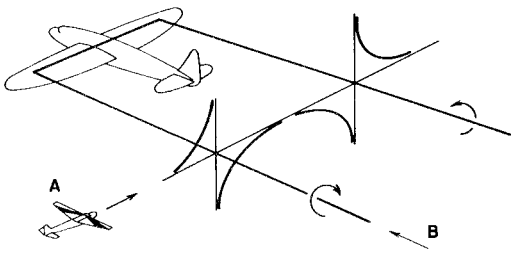

Fig. 3 Trailing vortex encounter.

diameter; heights may reach 70,000 ft. The thunderstorm is generally considered to yield the most severe turbulence, and at all costs is to be avoided. Cold fronts, Fig. 2d, consist of convective thunderstorm-type activity, and squall lines, Fig. 2e, consists of a series of thunderstorms stretched out along a path. Like the thunderstorm, the turbulence associated with cold fronts and squall lines can usually be expected to be severe. Along with identified locations of clear air turbulence, as through pilot reports, the thunderstorm, the cold front and the squall line are the major reasons causing aircraft to be diverted off of a normal or direct routing.

Hurricanes, Tornadoes, and Cyclones

These phenomena are, of course, producers of extreme turbulence. Since aircraft flight through these storms is generally always to be avoided, except in the case of special search planes for hurricanes, no further discussion is made here relative to them.

Wake Turbulence

This kind of turbulence, involving the strong trailing line vortices that are shed from the wing of an airplane in flight, is distinct from the others discussed up to this point in that it is "man-machine" made. These shed vortices can be quite strong, depending on the speed, weight, and span of the generating airplane, and can yield tangential or "gust velocities" exceeding 100 fps (Ref. 9). The main problems created by the trailing vortices are relative to the separation distance between aircraft during landing and takeoff at airports, the hampering or curtailment of certain military operations, and the hazards they create to light planes in general. Encounter can be basically of two types, Fig. 3. An encounter which crosses the vortices, path A, can create large loads in the encountering aircraft, while an encounter along the vortices as with a following aircraft, path B, can produce dangerous rolling moments.[10] A general notion has been that the larger the aircraft the more severe the trailing vortices, but this is not correct. Size alone is not the governing factor; rather strength and make-up of the vortices is governed by basic ratios, such as the weight-to-span ratio. Because of this fact, certain aircraft can generate vortices that are critical to one of its own kind. In the main, though, the problem involves smaller aircraft. Small aircraft encountering large vortices, in fact, do not have sufficient roll power to overcome the rolling power of the vortices and hence can be quickly rolled to extreme and even inverted positions. If the altitude is low, crash may follow before recovery can be made. One of the main problems of trailing vortices is that, like clear air turbulence, they can't be seen. Thus, much work is being carried out on the means for detecting them.[10] Much work is also being carried out on trying to understand the phenomena by which the trailing vortices break down or are dissipated and, in turn, what mechanisms might be used to enhance their breakdown. A primary goal in the study of wake vortices is to establish safe criteria for the separation of aircraft, both in time and in distance.

Severity Classification of Turbulence

In the United States and relative to aviation, turbulence is categorized in four intensities: light, moderate, severe and extreme. These categories, the associated aircraft reactions, derived gust velocities, incremental vertical accelerations, and frequently associated meteorological events were agreed upon by an industry and governmental group in 1967. Two convenient reference tables, one for the pilot and one for the forecaster, resulted from this group. Table 2, prepared on the basis of information contained in the tables and on response analysis work conducted by the author, is given as a way of numerically describing the four categories of severity.

Table 2 Classification of turbulence severity

	w, fps	$\sigma_{\Delta n}$	Δn	Wind shear fps/1000 ft	Clouds
	5	0.05	0.15	2.5	
Light					Cumulus
	20	0.2	0.6	10	
Moderate					Alto-cumulus, thunderstorms
	35	0.35	1.05	17.5	
Severe					Mature thunderstorms
	50	0.5	1.5		
Extreme					Severe thunderstorms

In this table w refers to an equivalent sea level velocity, $\sigma_{\Delta n}$ is a rms value for vertical acceleration, and Δn refers to peak vertical acceleration values. Additional description of the categories is also given by means of the following listing which was excerpted from the table prepared for pilot reporting.

Light: Occupants may feel a slight strain against seat belts or shoulder straps. Unsecured objects may be displaced slightly. Food services may be conducted and little or no difficulty is encountered in walking.

Moderate: Occupants feel definite strains against seat belts or shoulder straps. Unsecure objects are dislodged. Food services and walking are difficult.

Severe: Occupants are forced violently against seat belts or shoulder straps. Unsecure objects are dislodged. Food services and walking are impossible. Airplane may be momentarily out of control.

Extreme: Aircraft is violently tossed about and is practically impossible to control. Structural damage may occur.

Prediction or Detection of Turbulence

This section deals only briefly with means for predicting and detecting turbulence. Essentially, three different possibilities are involved: forecasting, pilot's reports of actual encounter, and remote sensing. The success or value of each of these methods is dependent on whether the turbulence is associated with visible formations or whether it is of the clear air variety. With respect to visible signs—convective clouds, thunderstorms, cold fronts, squall lines—there is no doubt that forecasting, weather map interpretations, and pilot reporting provide a positive and valuable service relative to the location of turbulence areas. The use of airborne radar has proved invaluable in locating areas to be avoided and in rerouting of flights so that turbulence encounter due to visible convective activity is kept to a minimum.

The situation with respect to clear air turbulence, however, is rather discouraging. Of the three categories for detection, only pilot reporting involving the passage of information on known turbulent encounter to other pilots is reasonably reliable. Forecasting may involve only a rough coverage, where indicators

such as surface wind magnitude, wind shear, wind flow strength over mountains, are examined, or it may involve detailed study of weather maps and even study of specific parameters such as lapse rate, wind gradient, and Richardson numbers in an attempt to predict where turbulence might be expected. At present, these predictions serve mainly only in the capacity of the "be alert for" type prediction.

Many studies on the remote detection of clear air turbulence have been made and are continuing. The various type systems studied include temperature, electric field, radar, lasers, ozone, optical, and consideration of general atmospheric variables. Although some of the systems have shown some promise in isolated instances, none so far has yielded the over-all reliable breakthrough that is needed.

Description of Turbulence

This section presents some of the basic expressions that are involved in mathematical descriptions and treatments of atmospheric turbulence. A more complete mathematical treatment of the structure of atmospheric turbulence may be found in several good books, Ref. 11 as an example.

An assumption commonly made is that atmospheric turbulence is isotropic, which means that there is no mean rate of transfer of momentum across shearing surfaces, or more specifically that the Reynolds or eddy shearing stresses, $-\rho\overline{uv}$, $-\rho\overline{vw}$, $-\rho\overline{uw}$, vanish, where ρ is density and where u, v, and w represent the longitudinal, lateral, and vertical turbulent velocities. In turn, the cross spectra between components ϕ_{uv}, ϕ_{uw}, ϕ_{vw}, vanish. Also, it is generally assumed that because of the rapid traversing, atmospheric turbulence may be regarded as a momentarily time frozen random surface in space relative to an airplane. The expression of gust histories and, in turn, statistical functions such as the auto-correlation function, in terms of either time or distance, is thus made possible through the transformation $x = Vt$, which represents a form of Taylor's hypothesis.

Certain key relations applying to isotropic turbulence are summarized in the following listing.

1-D Spectra:

$$\phi_u(L\Omega_1) = \int_{L\Omega_1}^{\infty} \frac{E(L\Omega)}{L\Omega}\left(1 - \frac{L^2\Omega_1^2}{L^2\Omega^2}\right) d(L\Omega) \tag{1}$$

$$\phi_v(\Omega) = \phi_w(\Omega) = \frac{1}{2}\phi_u(\Omega) - \frac{\Omega}{2}\frac{d\phi_u}{d\Omega} \tag{2}$$

$$\phi_w(\Omega) = \frac{1}{\pi}\int_{-\infty}^{\infty} R_w(x) e^{-i\Omega x} dx$$

1-D Correlation Function:

$$R_w(x) = \frac{1}{X}\int_0^X w(\xi)w(x+\xi)\,d\xi$$

$$R_w(x) = \int_0^{\infty} \phi_w(\Omega)\cos\Omega x\, d\Omega$$

$$R_w(x) = R_u + (x/2)\partial R_u/\partial x$$

Limit Values and Definitions:

$$\sigma_w^2 = R_w(0) = \int_0^{\infty} \phi_w(\Omega)\,d\Omega \tag{3}$$

$$\sigma_u = \sigma_v = \sigma_w \tag{4}$$

$$L = L_u = 2L_w = \frac{2}{\sigma_w^2}\int_0^{\infty} R_w(x)\,dx \tag{5}$$

$$\phi_w(\Omega)|_{\Omega=0} = \sigma_w^2 L/\pi$$

$$\phi(\omega) = (1/2\pi)\phi(f) = (1/V)\phi(\Omega) = (L/V)\phi(L\Omega)$$

$$\omega = 2\pi f = V\Omega$$

A few comments on these relationships may be made as follows. The one-dimensional spectrum ϕ_u is noted to be defined in terms of a general three-dimensional spectrum $E(\Omega)$: Ω is ω/V, where ω is circular frequency, and V is speed of flight. The vertical spectrum ϕ_w is noted to be expressible in terms of the longitudinal spectrum ϕ_u. The autocorrelation function R_w and the spectrum ϕ_w are Fourier transform pairs, but because they are both symmetrical can be expressed simply by cosine transforms, such as indicated for R_w. The functions R_w and R_u, as with ϕ_w and ϕ_u, are noted to be related by a differential expression, which is the result of the equation of continuity.

The area under the spectrum represents the mean-square value of turbulence. The initial value of the autocorrelation function by definition is also the mean-square value. The integral scale L is defined as twice the area under the R_w correlation function, normalized by dividing by σ_w^2. The initial value of the ϕ_w spectrum, using the frequency argument $\Omega = \omega/v$, is $\sigma_w^2 L/\pi$; this fact is often erroneously ignored or overlooked in deriving empirical equations for spectral shape.

The form adopted by von Kármán for $E(\Omega)$ was

$$E(\Omega) = C\frac{(\Omega/\Omega_0)^4}{[1+(\Omega/\Omega_0)^2]^{17/6}} \tag{6}$$

which exhibits an Ω^4 and an $\Omega^{-5/3}$ behavior at low and high frequencies, respectively, as was reasoned to be the situaton applying to isotropic turbulence.[12] The constants C and Ω_0 and the one-dimensional spectra that are obtained from this relation by Eqs. (1–5) are

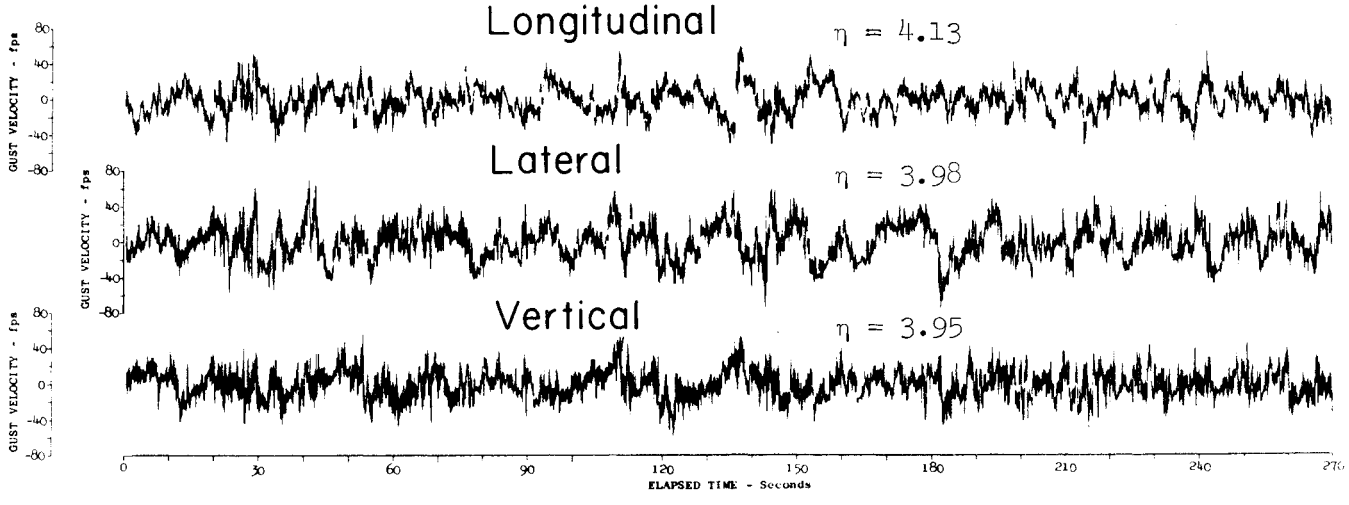

Fig. 4 Illustrations of measured turbulence velocities (severe).

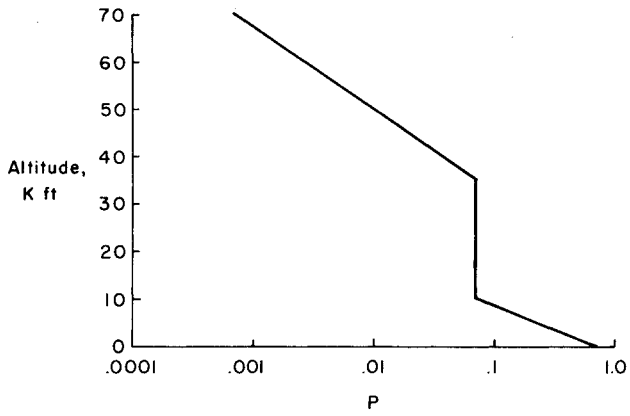

Fig. 5 Proportion of time spent in turbulence.

$$\phi_u = \sigma_u^2 \frac{2L}{\pi} \frac{1}{[1+(1.339L\Omega)^2]^{5/6}} \tag{7}$$

$$\phi_w = \sigma_w^2 \frac{L}{\pi} \frac{1+\frac{8}{3}(1.339L\Omega)^2}{[1+(1.339L\Omega)^2]^{11/6}} \tag{8}$$

$$C = (55/9)(L/\pi)\sigma_w^2; \qquad \Omega_0 = 1/1.339L$$

Specific items that are usually considered in the description of turbulence are the following: 1) Proportion P of time turbulence exists; 2) Spectral shape $\phi(\Omega)$; 3) rms turbulence severity values σ_u, σ_v, σ_w; 4) Integral scale length L; 5) Peak or level-crossing count of turbulence time histories; 6) Isotropy and homogeneity checks; 7) Effect of atmospheric variables. The influence of geographic location, season and altitude on these items is also of concern. The various items are discussed in the next section which deals with atmospheric turbulent measurements.

Measurements of Turbulence

In an attempt to understand the nature of atmospheric turbulence better, to provide data through which mathematical modeling of turbulence may be made, and to develop improved means for treating the response of aircraft in turbulent air, many experimental studies have been made, using fixed towers, balloons and aircraft probing. Many of the studies have been of the basic research type, while others are of the extensive data gathering type, such as the ALLCAT programs, which involves many individual projects aimed at searching for and sampling turbulence at all altitudes. This section gives a sampling of the various kinds of results that have been deduced from these measurements.

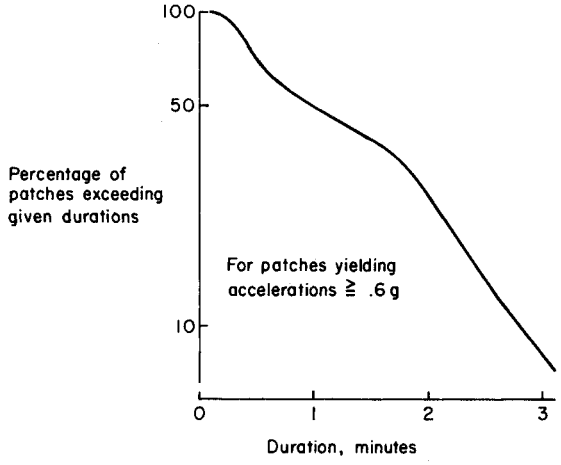

Fig. 6 Duration in turbulence patches.

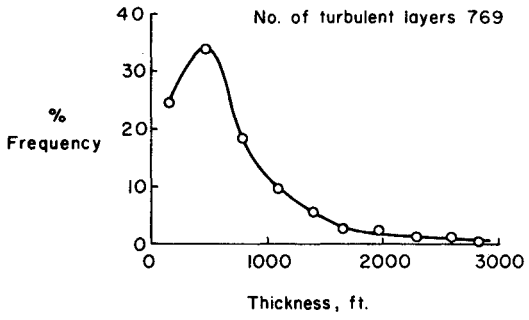

Fig. 7 Thickness of turbulence patches.

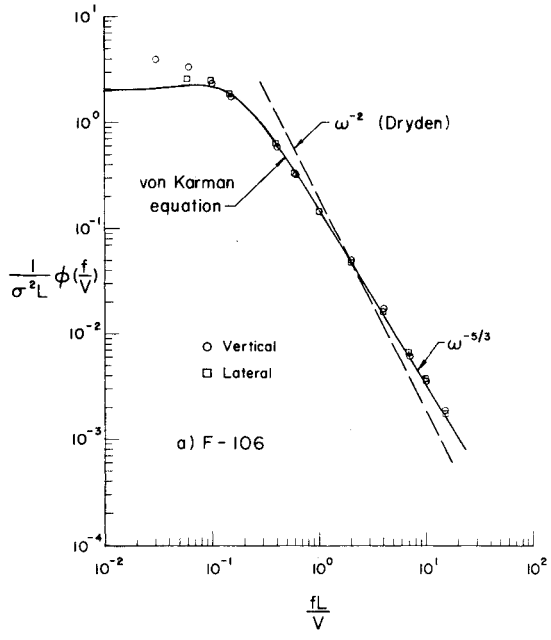

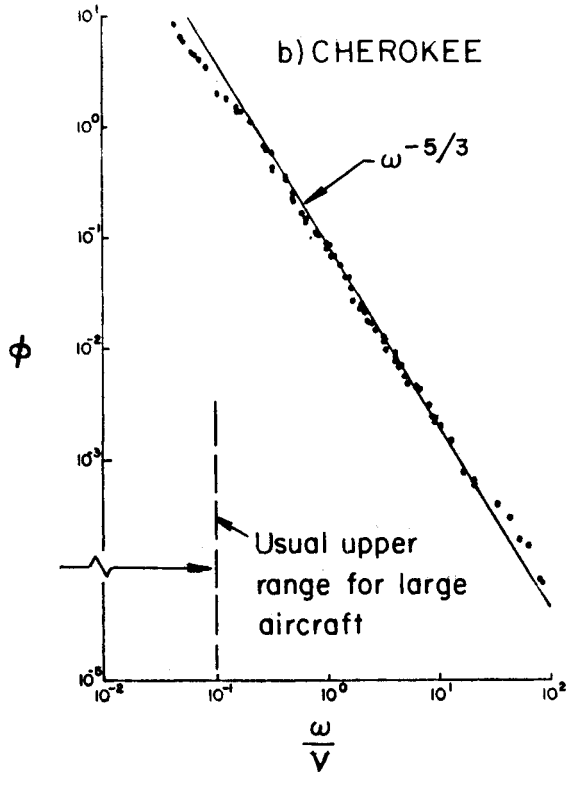

Fig. 8 Spectral shape of atmospheric turbulence.

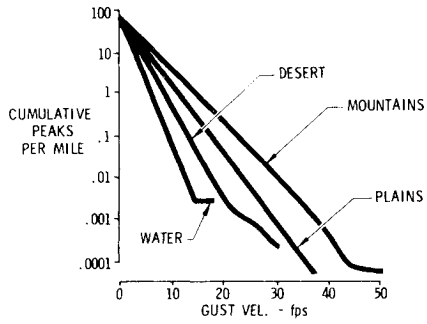

Fig. 9 Representative peak count curves.

Randomness

Figure 4 illustrates the nature, specifically the randomness, of the three components of turbulence that were deduced from measurements taken during flight through a patch of severe turbulence.[13] These time histories are representative of a well-established, fairly homogeneous turbulence situation. Often a variability in intensity is found to exist in a given turbulence encounter; that is, the severity may pass from light, to moderate, to light again. The values η listed in Fig. 4 denote the number of standard deviations (rms) that define the maximum gust velocity on each record. Examination of a number of such records indicated the maximum gust value on the record ranged from a low of around 2.7σ to a high of around 6.6σ, and that the average value of the maximum value appears to be in the range 4σ–5σ.

Extent of Turbulence Patches

Figure 5 indicates the proportion of time that turbulence may be expected, on the average, as a function of altitude. It would appear that this parameter is one of the easiest of all to establish, yet results obtained by different investigators differ by orders of magnitude. The results shown represent the best estimate that could be made by the author at this time. An indication of the size of turbulence patches is afforded by Figs. 6 and 7. The time required to traverse turbulence patches of moderate to severe intensity for worldwide civil aircraft operation is shown by Fig. 6 (Ref. 14). Statistical analysis of patch thickness yielded the results shown in Fig. 7 (Ref. 15). The majority of patches are seen to be quite shallow.

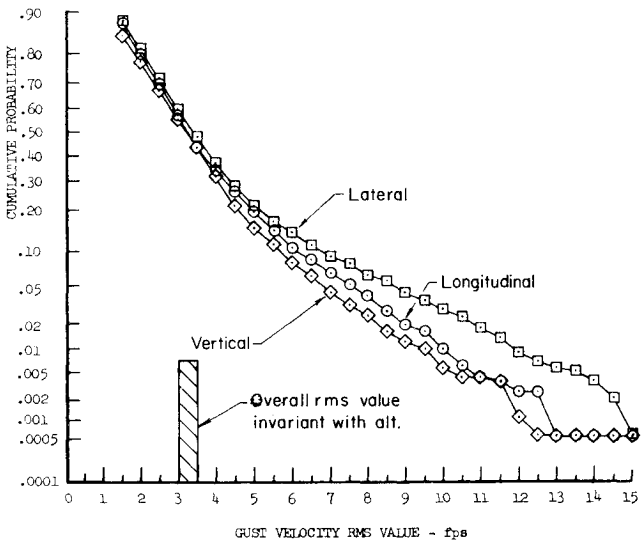

Fig. 10 Cumulative probability of rms gust velocities.

Spectral Form

Typical results of the power spectra that are deduced from measured turbulence velocities are shown in Fig. 8. Part a represents results obtained from F-106 flights.[16] Earlier statistical treatments of atmospheric turbulence usually employed a spectral shape due to Dryden for mathematical modeling purposes. This spectrum, based on exponential curve representations of the correlation functions for turbulence velocities, exhibits an ω^{-2} fall off at high frequencies. More recent studies have concentrated on the use of the spectrum equation due to von Kármán, Eq. (8), which exhibits an $\omega^{-5/3}$ fall off at high frequencies. The solid curve in Fig. 8a is given by this equation. Figure 8b gives spectral data as deduced from turbulence measurements made by use of a Cherokee aircraft.[17] These data represent spectral information in a frequency range three orders of magnitude beyond that obtained by large aircraft; in this case vane measurements of turbulence velocity could be used directly without having to subtract out airplane motion effects, as is necessary with large airplane probing covering the low frequency range. The line in Fig. 8b represents the $\omega^{-5/3}$ variation of the von Kármán equation. Both parts of Fig. 8 indicate that the von Kármán equation is the preferred form for modeling purposes; this observation appears to be the consensus.

Peak Count

Figure 9 is representative of peak count curves that have been derived from time histories of turbulent velocities.[14] The trend shown relative to the effect of terrain on peak count is typical, and reflects the difference in turbulence generation mechanisms depicted by Fig. 1.

Turbulence Severity

A common means for representing severity of turbulence patches is in terms of the rms value of the velocities sensed. Representative probability curves associated with rms severity are shown in Fig. 10 (Ref. 13). The larger rms values, approaching 15 fps, though rare, are of special interest since they are significant to the design strength of aircraft. The 4σ value of a

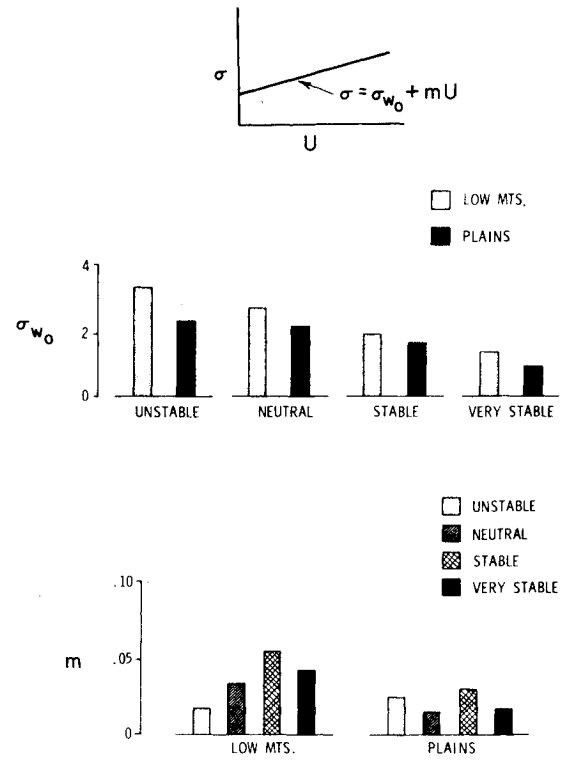

Fig. 11 Effect of atmospheric stability and winds on rms gust values.

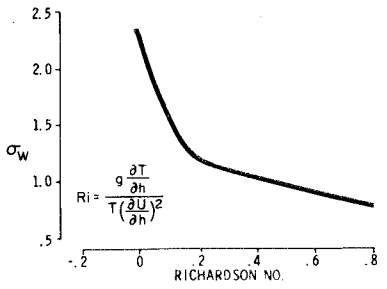

Fig. 12 Gust severity variation with Richardson number.

patch having a rms value of 15 fps, for example, is 60 fps, which is equivalent to the values used for gust design purposes. The more frequent patches of lower rms value are of significance to the structural fatigue problem. The rms value of all turbulence encountered, giving due regard to the proportion of time that patches of various severity are found, appears to be essentially invariant with altitude and is in the range of 3–3.5 fps. It is to be noted that, in contrast to many random processes, atmospheric turbulence represents a random process in which the maximum values of gust velocities are on the order of 20 times the over-all rms value, even though maximum values in any individual patch are on the order of 4 times the rms value for the patch.

An interesting example of the turbulence velocities that were found to exist in a short isolated severe turbulence is that of an incident involving a B-52 airplane flying at about 14,000 ft on the lee side of the Spanish Peaks of Colorado[18]; the encounter was abrupt and resulted in the fin and rudder being torn from the airplane. The pilot managed to maintain control of the airplane and proceeded on to a successful landing. Subsequent analysis of airplane motion records indicated that gust velocities in both the vertical and lateral direction approached 80 fps, and that differential vertical gust velocities between the right and left wing tips were as high as 60 fps. The nature of the vertical, lateral and roll components, and their phasing, indicated that the incident was probably that of a severe rotor encounter, Fig. 1c.

In the ALLCAT program attempts were made to relate turbulence severity with atmospheric parameters, such as winds and atmospheric stability. Results obtained indicate that turbulence severity tends to be linearly related to wind speed, U and specifically suggest an equation of the type

$$\sigma_w = \sigma_{w_0} + mU$$

Figure 11a shows example results that were obtained for σ_{w_0}, as dependent on atmospheric stability[14]; a trend is indicated of increasing turbulence intensity with decreasing atmospheric stability. Part b gives sample results for the slope m. This slope parameter appears to be larger in general for rough terrain than for plains. Interestingly, the largest slope values seem to occur when the atmosphere is classified as stable.

If solar radiation is strong, then it might be expected that turbulence intensity is more dependent on the convective currents than on wind shear. Results obtained from measurements made over North Africa indicate, in fact, that mean-square turbulence intensities were directly proportional to solar radiation.[19]

The Richardson number, which involves the ratio of the rate at which work has to be done against gravity by the turbulence to the supply of energy made available by the Reynolds stresses, is often examined for possible correlation with turbulence intensities. The number is often defined in various forms, but a common form is

$$R_i = \frac{g\,\partial T/\partial z}{T(\partial U/\partial z)^2}$$

where T is potential temperature and U is the mean wind speed. Representative statistical results showing the correlation between rms gust velocities and the Richardson number are shown in Fig. 12 (Ref. 14). These and other analyses indicate a significant probability of encountering turbulence at Richardson numbers less than one, and that severity tends to rise abruptly for numbers less than 0.2. In general, however, too much is expected of the Richardson number. The general equations of fluid motion contain many other terms besides the shear and buoyant force terms making up the Richardson number, and these may be large relative to the Richardson number terms. These other terms can therefore be expected to have a large influence on the severity of the turbulence being generated, dependent on whether the turbulence state is one of production, stability or dissipation, and only where a reasonable balance has been obtained between shearing forces and gravity or buoyant forces can the Richardson number be expected to apply.

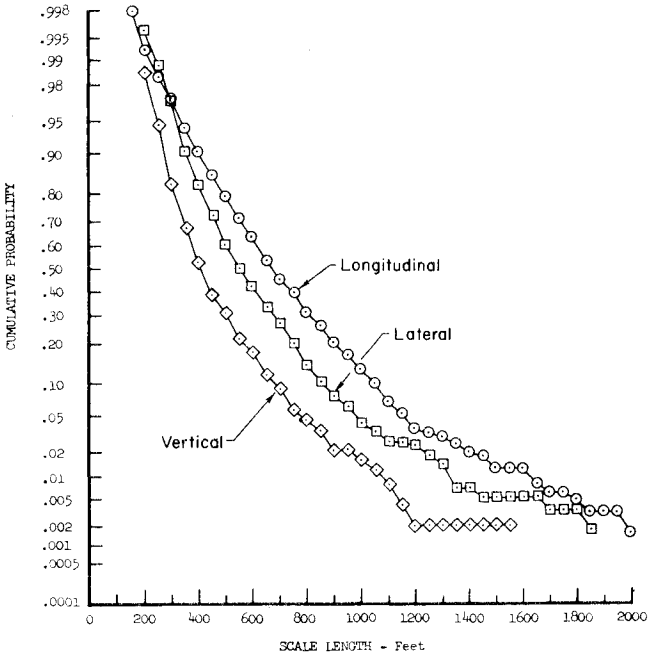

Fig. 13 Cumulative probability of integral scale values.

Integral Scale Values

Intimately associated with the severity and spectral shape of turbulence data is the integral scale of turbulence L, as defined by Eq. (5) and appearing in Eq. (7). Representative statistical results for deduced scale values are shown in Fig. 13 (Ref. 13). Mean values showing the influence of atmospheric stability are shown in Fig. 14. These figures indicate, at least for the altitude of flights represented, a mean value of scale in the 500–700 ft range. There is some indication that scale value may increase as turbulence severity increases. Figure 15 shows results relative to this question. The scatter is great, but a rough trend indicating that scale length grows as severity increases is perhaps present.

Estimates of the value of scale applying to atmospheric turbulence may be made by considering the values of scale that are found in carefully controlled laboratory tests of various phenomena. An open jet, for example, indicates an integral scale value of about 0.5 of the reference radius, where this radius is defined as the point where the mean velocity profile has dropped to one-half the maximum or centerline velocity. The diameter d of the area of air that is affected to any significant extent by the jet is in the order of 4 times this radius; these numbers suggest that the relation $L = d/8$ might serve as a rough rule of thumb for estimating scale. The application of this rule of thumb to turbulence-producing phenomena of the atmosphere, such as large Benard cells 0.5–1 mile in diameter, thunderstorm cells on the order of 1 mile in diameter, turbulent shear layers of about 4000 ft thickness, yields estimates of scale values for the atmosphere of from 300–700 ft. By contrast, many quoted values of scale are in the 2500–3000 ft range. The author feels that more research will indicate that the lower values rather than the higher values are more realistic, but realizes that this belief is open to much controversy.

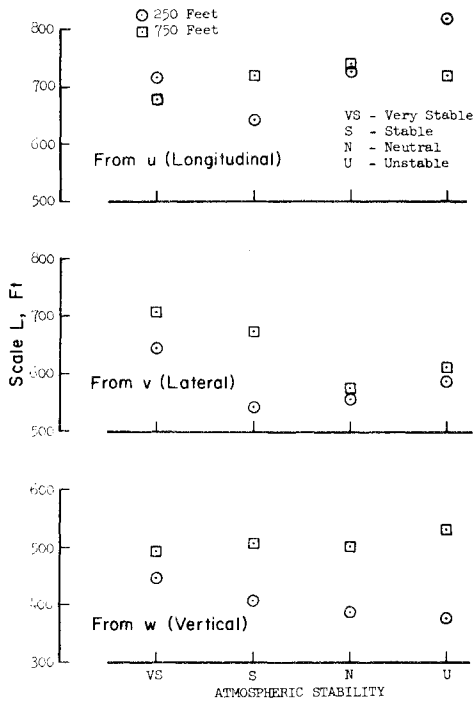

Fig. 14 Effect of atmospheric stability on mean scale value.

Isotropy, Stationarity, and Homogeneity

A general assumption made in aircraft response studies is that atmospheric turbulence is isotropic. Measured data are often examined to check on this assumption. Theory shows that in terms of the von Kármán spectral function, the ratio of longitudinal spectrum to the lateral spectrum should give results of the type shown in Fig. 16a. Data checks made yield results which are in rough conformity to the curves shown in this figure, more so at the high-frequency end, where the ratio is simply a constant value of 0.75. Another check on isotropy is through means of the coherency functions between the three basic components of turbulence. Isotropy implies that the Reynold's shearing stresses vanish, and hence so do the cross spectra between the turbulence components. This means that the coherency function also vanishes. Defined in terms of the u and w components, the coherence function is

$$\gamma_{uw}^2 = |\phi_{uw}(\Omega)|^2/\phi_u(\Omega)\phi_w(\Omega)$$

where ϕ_{uw} represents the cross spectrum between the u and w components, and ϕ_u and ϕ_w represent the power spectra. Typical results as derived from measured data are shown in Fig. 16b (Ref. 14). These results, as well as results for the covariance values (the time average values of the products vw and vu, for example), indicate that, from a practical engineering point of view, atmospheric turbulence may be treated as being isotropic. In laboratory experiments of classical shear flow typical values of covariance are found to be

$$\overline{uw} \cong 0.15(\sigma_u^2+\sigma_v^2+\sigma_w^2)$$

By contrast, values for atmospheric turbulence appear well below such levels, thus supporting the isotropic concept.

The properties of stationarity and homogeneity of a random process specify an invariance in the statistical characteristics of the process with respect to position along the time history where the sampling is taken. Checks for these properties with respect to atmospheric turbulence have generally been made by taking a derived time history, dividing the record into halves or thirds, and then establishing such quantities as the rms value and spectrum of each portion. The results obtained indicate that generally there is homogeneity with respect to spectral shape content and that, in some cases, there is stationarity with respect to rms severity; in other cases, rms severity varies from section to section along the time history, as might be expected. It should be noted that if the turbulence is locally stationary with respect to time, then, in accordance with Taylor's hypothesis, homogeneity in space will be found.

Uncertainties in Data Processing

The processing of turbulence data involves some uncertainties with respect to procedure and subsequent interpretation. This section discusses briefly some of the less commonly known uncertainties; some of those discussed are, in fact, controversial in nature.

One question that arises is with respect to whether the turbulence being sampled also reflects some of the information on the over-all phenomenon creating the turbulence, or whether the over-all phenomenon might be changing during the duration of the sampling. Two examples are given by way of illustration. Consider a freejet, Fig. 17, and consider the data that are obtained by moving a probing sensor across the jet. If the measurement is processed intact, that is, with the mean profile included, then a spectrum such as represented by curve a would result. If the mean profile is removed from the measurements, however, the

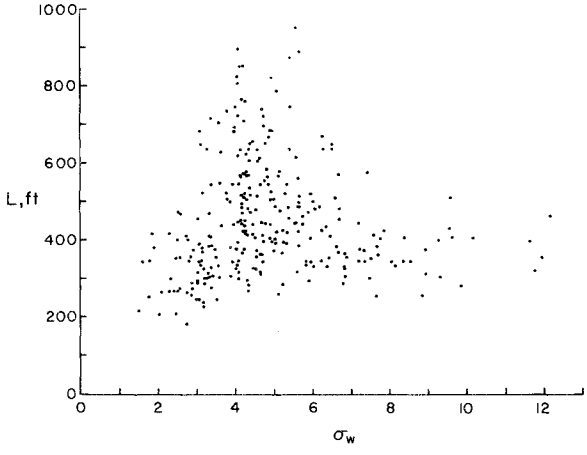

Fig. 15 Correlation of integral scale with rms gust severity.

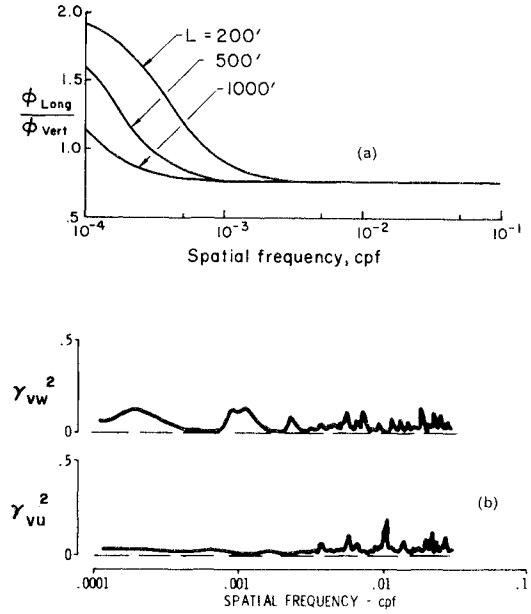

Fig. 16 Measures of isotropy.

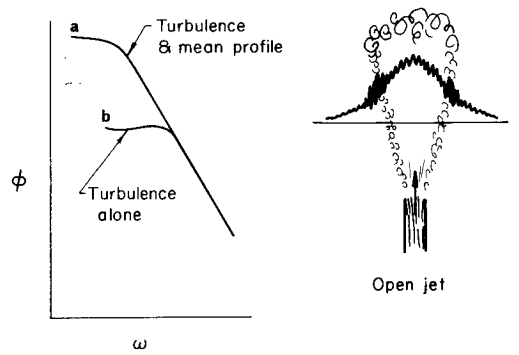

Fig. 17 Effects of mechanisms producing turbulence.

result would be more like curve b. Results obtained and subsequent interpretation are thus quite dependent on the processing made.

The second example relates to the range of scales of atmospheric motions which have an effect on aircraft operation. The largest or global scale is the air motion associated with "the existing weather." When this "global weather" picture is considered, it may be noted that the scale of turbulence, as established by the winds, is so large that aircraft would sense mainly steady wind patterns. The length of the "waves" in the wind pattern is of the order of thousands of miles, so the frequency of wind change as seen by the airplane is in terms of a fraction of a cycle per hour. The over-all pattern of wind "turbulence" affects aircraft navigation only, and does not affect aircraft loading or stability and control. If an extremely high fast vehicle is imagined to cross the wind pattern, however, then the same waves will appear as comparatively fast changes, and possible effects on stability and control, and perhaps loads may result. Thus, from the viewpoint of flight of aircraft, turbulence "scale" has a relative meaning, and what is essentially a steady-state condition in one case could be a rapidly varying condition in another case.

The influence of the notion of area extent of sampling or of time of sampling can be invisaged in terms of sampling atmospheric turbulence over different intervals of time. Different spectra of "turbulence" will be obtained according to whether the interval is on the order of minutes, hours, days, weeks, months, or years.[20] Thus, the spectra obtained, and the severity and turbulent scale values which are indicated, are strongly dependent on what components of velocity are considered as turbulence.

Figure 18 illustrates a problem that is encountered in deducing

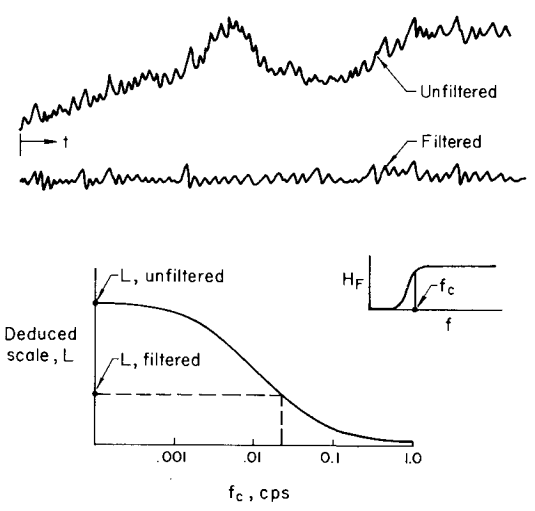

Fig. 18 Effect of filtering on integral scale.

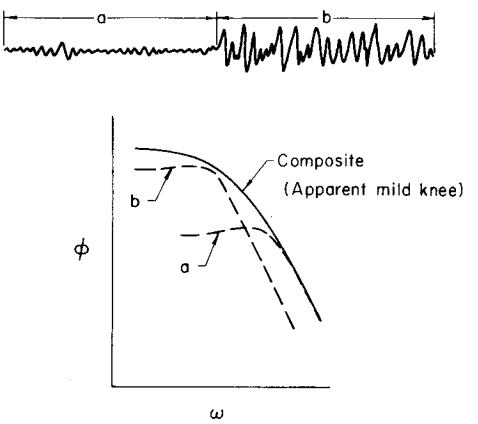

Fig. 19 Effect of nonhomogeneity on spectral shape.

the integral scale L of turbulence [as appearing in Eqs. (7) and (8)] from measured velocities. Generally, in aircraft probing of turbulence, gust velocities have to be derived from an equation which takes into account airplane motion effects, such as the following equation for vertical gust velocities:

$$w = V\alpha + \int \dot{z}\,dt - V\theta + e\dot{\theta}$$

Thus, the effects of vertical motion $\dot{z}$, pitch attitude θ, and pitch rate $\dot{\theta}$, must be subtracted from the angle of attack or gust vane measurement α to yield the derived gust velocity w. The velocities that are derived, however, usually exhibit a large content of low-frequency noise or hash, because of instrumentation drift and numerical integration errors, such as arise in establishing aircraft vertical velocity by integration of aircraft vertical acceleration. A typical gust velocity may appear, for example, as shown in the top of Fig. 18. To remove the low-frequency noise, a high pass filtering is usually made, leading to a filtered time history, as depicted by the lower time history on the figure. From this filtered time history, a spectrum, rms severity, and integral scale value are deduced. Unfortunately, the effect of filtering on the deduced scale values is not fully understood. Reference 21 examines the problem and indicates results of the type shown on the bottom of the figure. It is seen that it is difficult to ascertain what the correct scale value might be, because of the monotonic manner in which scale value drops off as filter cutoff frequency is increased. A discussion of various filtering techniques and other effects is given in Ref. 22.

Nonstationarity of gust velocities records also gives rise to uncertainty in derived spectral results. Consider the time history shown in Fig. 19. If the portions of small and large severity were analyzed separately, spectral curves a and b would result, each of which would be represented well by the von Kármán spectrum, Eq. (8). Analysis of the combined record, however, leads to the composite spectrum shown. This composite spectrum exhibits a "mild knee" variation, as contrasted to the sharper distinct knee of the von Kármán spectrum. The apparent mild knee behavior of such composite spectra has caused some investigators to search for equations other than the von Kármán equation for mathematical modeling purposes. This search, which is perhaps improper or without adequate basis, has created additional problems, as brought out by the results shown in Fig. 20. This figure is prepared on the basis that spectral data at high frequencies and the rms value of a gust velocity time history are known. These data are fitted by two curves, one as indicated by the von Kármán equation, the other a mild knee type equation given by

$$\phi(\Omega) = (\sigma^2 L/\pi)\,1/(1+0.477L\Omega)^{5/3}$$

It is seen that, to fit the same data, the von Kármán relation yields a scale L of 700 ft, while the mild knee expression indicates a scale of 2100, a factor 3 different. Differences of this type have led to much confusion with respect to quoted scale values. One

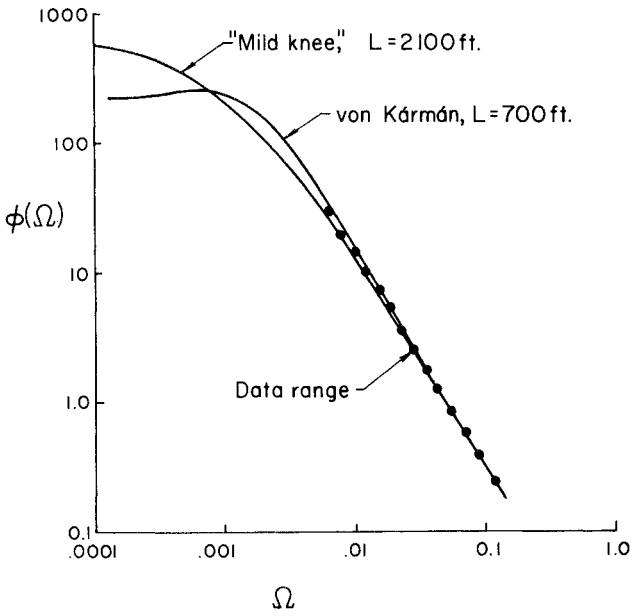

Fig. 20 Influence of spectral equations on deduced L value.

must thus be careful in comparing the scale values obtained by one investigator using one form of spectral function with the scale values obtained by another investigator using a different function.

Because of the confusion which exists with respect to filtering and derived integral scale values, the author has attempted to develop other means for sampling turbulence.[23] A possible scheme is shown in Fig. 21. The probe is simply a two sensor configuration measuring longitudinal fluctuations. The recording of the difference of the two signals gives a result which has all airplane motion automatically removed. Theoretically, the spectrum of the recorded signal should appear as shown by the curves in the figure, where normalization of the peak value to unity has been made. The procedure for measurement and analysis is thus simply: a) record the difference of the two signals, b) establish the spectrum of this difference, and c) plot the results on the figure and read off the scale value by interpolation. A feature of the scheme is that it involves mainly the use of

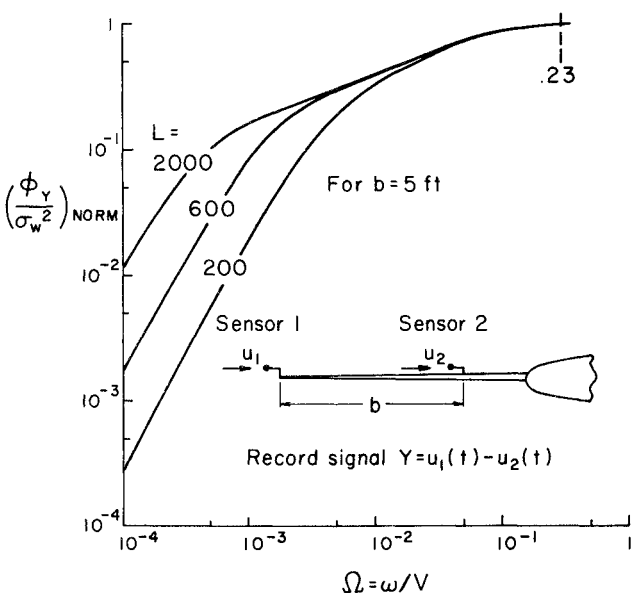

Fig. 21 Two-sensor system for direct measurement of turbulence.

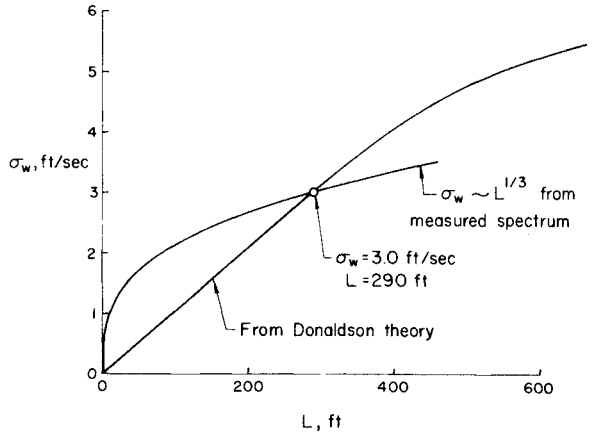

Fig. 22 Combined theory-experiment for determinations of scale.

information in the frequency range where low-frequency noise is not a problem.

Another possible scheme for deducing integral scale value and turbulence severity is that suggested by Donaldson.[24] In this reference, treatment is made of turbulent shear flows by an invariant modeling closure of the equations for the second-order correlations of fluctuating quantities in a turbulent medium. With the equations, and knowledge of the vertical mean wind and temperature profiles, Donaldson shows that a relation between rms severity and integral scale can be derived. In addition, Ref. 12 shows that, in dealing with partial spectral data, the most that can be said is that the rms severity is equal to a known constant time $L^{1/3}$. Combination of these two relations leads to results of the type shown in Fig. 22, which applies to a particular case studied. The intersection gives both the rms severity value and the integral scale.

Aircraft Response and Loads Analysis

This section presents some of the highlights that are involved in response treatments of aircraft to atmospheric turbulence encounter. Emphasis is given to the spectral approaches.

Discrete Gust and Spectral Approaches

The earliest gust loads studies were in terms of the concept of a single or discrete-gust encounter, where the gust shape was considered to be of the sharp-edged or step function type. Later, the concept was modified to incorporate a specified profile discrete gust. Figure 23 gives the main notions behind the discrete-gust approach that has been used for years for establishing gust loads on aircraft for design purposes, and which is still in partial use today. Essentially, the peak vertical accelerations that were measured on airplanes flying in gusts were analyzed to

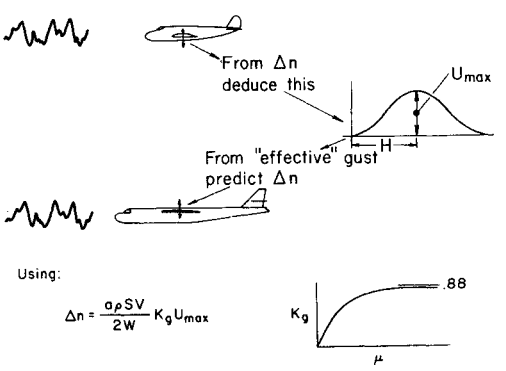

Fig. 23 Discrete-gust approach to design.

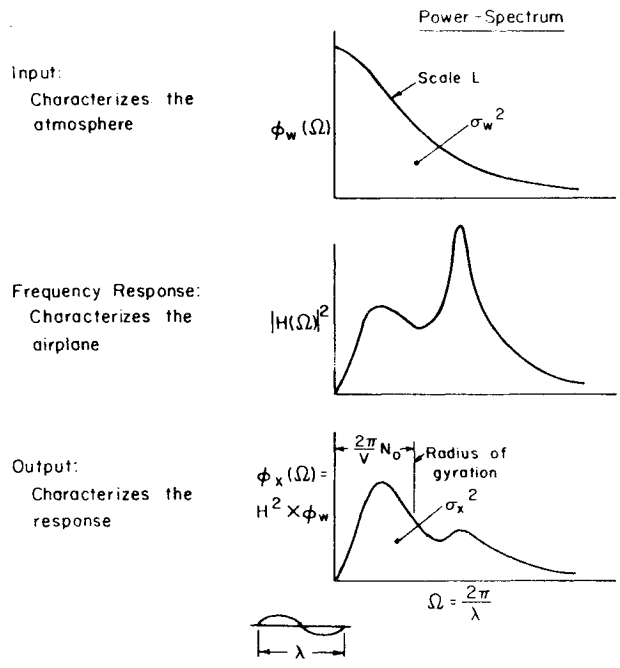

Fig. 24 Input-output relations for gust response.

derive gust gradient distances H and the severity values U_{max} as though each acceleration value came from an isolated discrete gust of fixed shape. These "effective" gusts are then used as a means for establishing the loads that could be expected on a new design. The commonly quoted design values of $U_{max} = 50$ fps, and $H = 8-12$ chords resulted from this procedure. The shape that has been adopted for years is the 1-cosine shape. The reason behind this choice is somewhat obscure, but appears to be connected with the view that no gust could start with a finite slope, a notion which is quite irrelevant and minor as compared with the basic and rough assumption which forms the base of the concept, namely, that realistic gust encounter could be represented by discrete gusts. Actually, any shape such as a half sine wave, a triangle, or even a sharp edge gust would have worked just as well.

During the past 20 years, great strides have been made in developing the spectral technique for designing aircraft for gust encounter.[25-28] The essentials of the problem are shown in the rather popular presentation represented by Fig. 24 (Ref. 26). A basic assumption made in spectral applications is that Taylor's hypothesis applies, namely, that time histories of gust velocities obtained from aircraft may be converted to space fixed "temporarily frozen," space histories. Another assumption usually made is that the gusts are random in the flight direction only, but are considered uniform in the spanwise direction; this assumption is based on the notion that the scale of turbulence L is large compared to the airplane dimensions.

The basic spectral procedure involves choosing a spectrum for gust velocity input, Eq. (8), a scale value L, a rms gust severity value σ_w, and then through the frequency response function to derive the output response spectra, from which two basic structural parameters A and N_0 are found as defined by the following equations

$$A = \left[\int_0^{\omega_c} |H(\omega)|^2 \phi(\omega) d\omega \Big/ \sigma_w^2 \right]^{1/2} \tag{9}$$

$$N_0 = \frac{1}{2\pi} \left[\int_0^{\omega_c} \omega^2 |H(\omega)|^2 \phi(\omega) d\omega \Big/ \int_0^{\omega_c} |H(\omega)|^2 \phi(\omega) d\omega \right]^{1/2} \tag{10}$$

Basically, A is the proportionality constant relating the rms value of the chosen output parameter of concern, σ_x, to the rms value of gust severity, or $\sigma_x = A\sigma_w$; and N_0 denotes the number of times per second the output response crosses the mean 1-g load level value of x with positive slope.

Frequency Response Function for Gusts

With reference to Eqs. (9) and (10), the determination of the frequency response function H, defined as the response of the variable x due to a unit sinusoidal gust, and involving the combined considerations of the structural dynamics and nonsteady aerodynamics of the airplane configuration, is fundamental to the spectral approach. Although evaluation is quite complicated, it appears that reasonable practical success is achievable in the determination of H. Figure 25 gives two cases showing a comparison between theoretically and experimentally derived H-functions. Part a shows fairly good agreement and indicates that at least some flexible modes are needed in addition to the two rigid modes of vertical translation and pitch. In part b, the agreement is good at low frequencies, but is less so at high frequencies. Fortunately, the higher frequency end does not show up significantly in the output spectrum.

The establishment of N_0 is often a problem since, in many cases, the integral of the numerator does not appear to converge with increasing ω_c values. A recommended way for treating such cases is to make a plot of A as a function of ω_c; the value of ω_c associated with the "top of the knee" of this A plot is then used as the ω_c values for establishing N_0.

Structural Design Procedures

If the airplane is assumed rigid and is considered to have the degree of freedom of vertical motion only, it is possible to derive spectral results in simple convenient chart form, which are exactly analogous to the discrete gust concept, thus permitting a quick

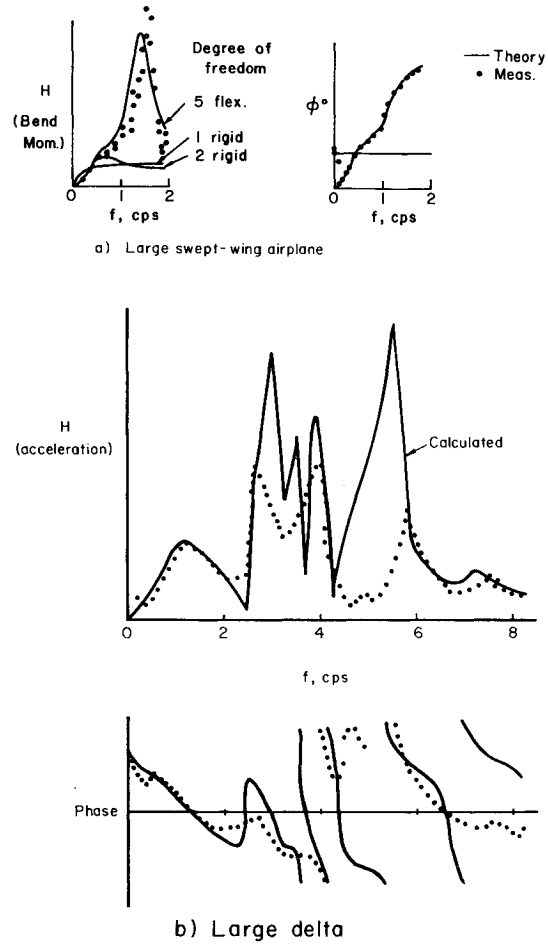

Fig. 25 Calculated and measured frequency response functions.

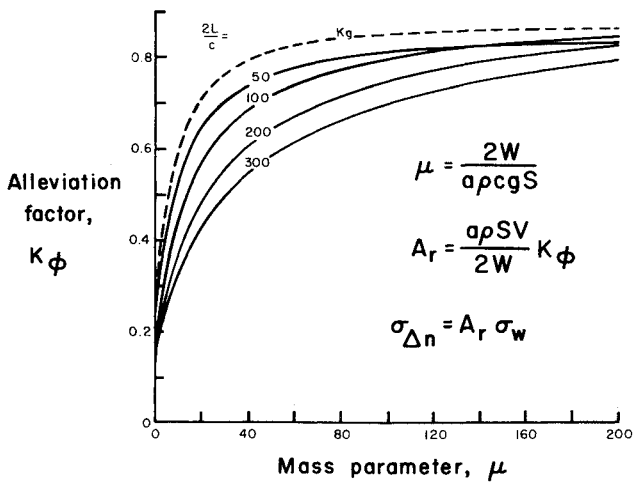

Fig. 26 Spectral results for rigid airplane.

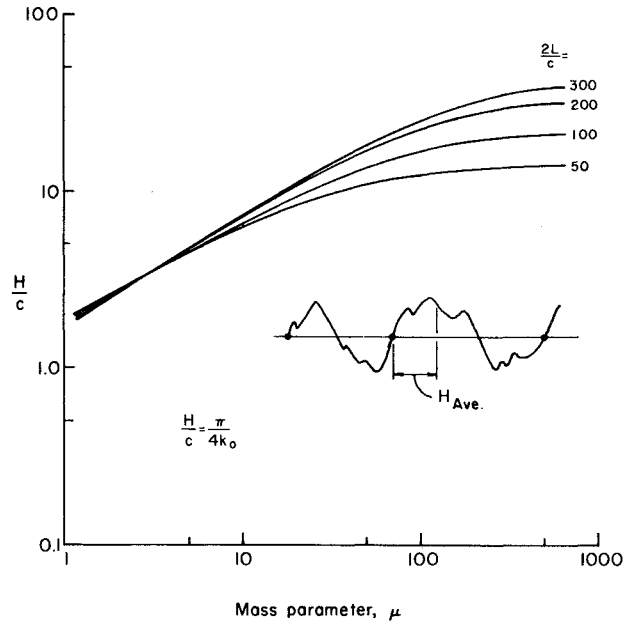

Fig. 28 Effective gust gradient distance as given by spectral approach.

rough estimate of c-g accelerations to be made.[26] Results are summarized in Figs. 26 and 27.

Figure 26 leads to A_r, the A value for rigid body vertical acceleration; a is the lift curve slope, ρ air density, S wing area, V velocity, W weight, and K_ϕ is the spectral alleviation factor as established by the mass parameter μ, the scale L and mean cord c. The alleviation factor K_g as obtained by the discrete-gust treatment is shown also on the figure for comparison. Figure 27 yields the parameter N_0. A rigid body treatment which also investigates the influence of compressibility effects on the alleviation factor is described in Ref. 5. It is to be noted that a very simple spectral design procedure, exactly analogous to the discrete-gust design approach, can be stated in terms of Fig. 26. Reference 26 indicates that peak values of gust velocity of about 55 fps in the spectral approach correspond to the 50 fps of the discrete approach. This equivalence suggests the following equation for incremental design load factor for a simple spectral approach

$$\Delta n = 55 A_r$$

where A_r is obtained from Fig. 26.

The value N_0 is, in effect, one-half the average number of zero crossings that occur per second. The equivalent of an average effective gust gradient distance that is indicated by this frequency is $H = \lambda/4$ where λ is V/N_0; the values of H computed in this manner from the results in Fig. 27 are shown in Fig. 28 (Ref. 26). It may be conjectured that this figure, based on spectral considerations, may offer an explanation of why a predominance of gust gradient distances of around 10 chords was found in early discrete-gust studies. The airplanes used then were quite rigid and had a mass parameter μ of around 20; for this value of μ, Fig. 28 indicates a H/c of around 10, in surprising conformity with the discrete gust results. The spectral approach thus appears to confirm that the discovery of gust gradient distances of a distinct nature in earlier discrete-gust studies was logical.

Numerous attempts have been made to derive generalized load exceedances curves based on the power spectral approach, and while there is general agreement on their nature, there is disagreement on what their specific values should be. Reference 25 shows the general theoretical development of exceedance curves in the form N/PN_0 vs x/σ_A, where N refers to the number of exceedances per second, P refers to the proportion of time spent in turbulence (see Fig. 5), x refers to the incremental value that is due to gusts of the response parameter that is being considered, such as bending moment, σ denotes the over-all rms gust severity value, and A and N_0 are the structural response quantities as given by

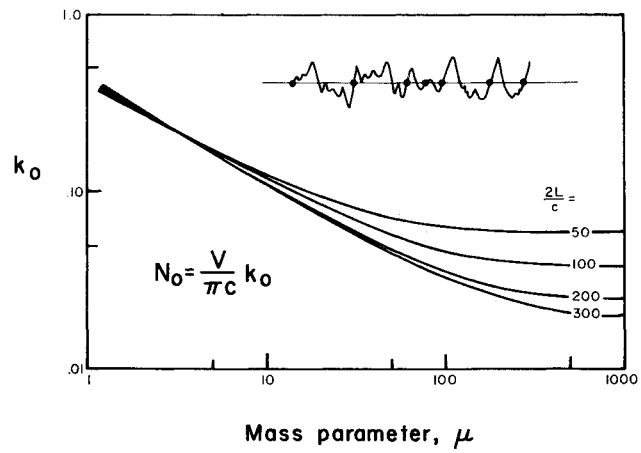

Fig. 27 N_0 values for rigid airplane.

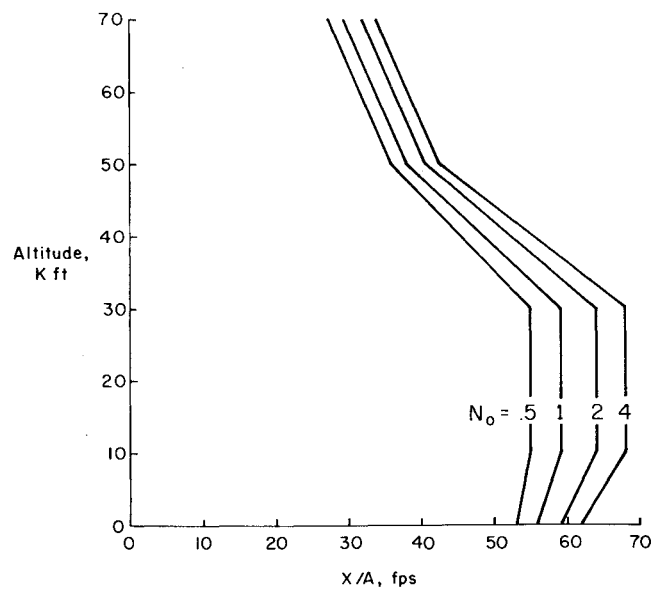

Fig. 29 Gust design borders for simplified approach.

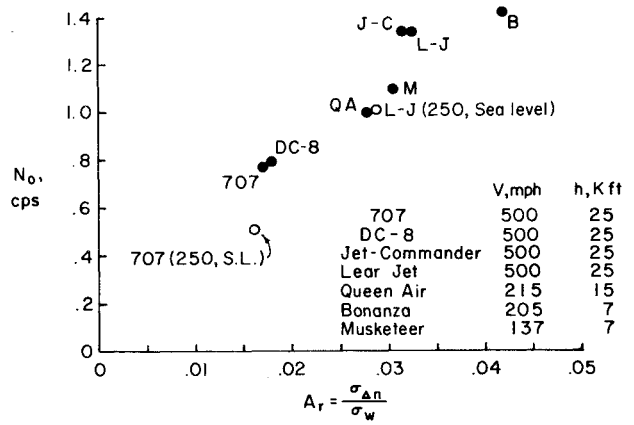

Fig. 30 Illustrative A_r and N_0 values for several aircraft.

Eqs. (9) and (10). In Ref. 25, it is shown that the assumptions of stationarity and Gaussian properties for gust processes, as usually made, are not essential. The curves thus automatically take into account the nonstationary and non-Gaussian nature of the over-all atmospheric gust process, even though local patches of turbulence may exhibit stationary and Gaussian properties.

If P and σ are specified, the generalized exceedance curves may be converted directly to simple design curves of the form N/N_0 vs x/A. Reference 26 presents such curves; these curves are presently being updated on the basis of further extensive data that has been obtained. A basic design approach is to use the N/N_0 vs x/A curves in a detailed way that is based on mission considerations. Design is made on the basis that the composite N as obtained from the assumed mission or missions does not exceed a stipulated value at the limit load value for x. The only parameter that has to be specified in such an approach is the scale L; the value suggested for L is 800 ft for all altitudes.

A simpler design procedure can be stated, based on the concept that the value of N should never be greater than a stipulated value, regardless of the altitude of flight. A value of N that appears consistent with past design practices is $N = 5 \times 10^{-8}$. Typical design borders involving only x/A as a function of altitude as obtained with this value of N and a chosen set of N/N_0 vs x/A curves are shown in Fig. 29. Safe design is indicated if the x/A values for the airplane under evaluation fall on or to the right of the appropriate N_0 curve.

Figure 30 is given to indicate the rigid body A and N_0 values that are found for several different airplanes, and to show the relative ride comfort of these airplanes in rough air. The solid points for jets apply as though they were flying side by side at 500 mph at 25,000 ft in the same rough air. Nominal cruise velocities and cruise altitudes were chosen for the smaller aircraft shown. The larger A is, the rougher the ride; the larger N_0 is, the more "jolts" per second. It is seen that the 707 and DC-8 have smoother riding characteristics than the smaller jets, and that ride qualities of the small airplanes, particularly the Bonanza, are relatively rough. The open points compare the 707 and Lear Jet at 250 mph at sea level, and also how their characteristics compare with faster flight at altitude. The 707 is again seen to offer smoother riding qualities.

Nonuniform Spanwise Gusts

This section discusses the problem of gust encounter wherein the gusts are considered random in the spanwise direction, as well as in the direction of flight, as depicted in Fig. 31. This case may be of significance for large flexible aircraft where the span may become an appreciable fraction of the scale of turbulence. In these circumstances, it is possible for some of the modes, particularly the antisymmetrical and higher frequency modes, to be excited to a much greater extent than they would be in the case of uniform spanwise gusts. The over-all response for the completely random gust environment may thus be larger than for the environment which is considered random only in the flight direction. The gust encounter incident of a B-52 described in Ref. 18 is a situation where it seems fairly clear that the gusts were markedly nonuniform in the spanwise direction. Also, it might be expected that if the scale of turbulence is around 600–800 ft, then significant spanwise effects could result for airplanes having spans in the order of 300 ft.

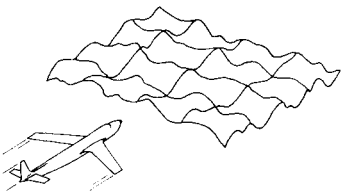

Fig. 31 2-D gust encounter.

A general means for treating the case of nonuniform spanwise gust and some example results are given in Ref. 29. Additional notable treatments are represented by Refs. 30 and 31. Essentially, the problem is that of a system being excited by multiple random inputs rather than by a single one. Cross spectra between the individual inputs must therefore be considered, along with the spectral value of each input. Figure 32 shows the cross spectra that have been developed for isotropic turbulence, as based on Eq. (8) (Ref. 32). The means for using the results given in this figure in gust response calculations are quite straightforward, and involves mainly an increase in computational effort. The basic procedure described in Ref. 29 is essentially as follows. The wing is first divided into equally spaced spanwise segments, say from 6 to 10. Frequency response functions for the response variable of concern are then derived for each of the segments, assuming that the unit sinusoidal gust is uniform over the segment being treated. The output response spectra then follows by the equation

$$\begin{aligned}\phi_x = {} & \phi_0[|H_1|^2 + |H_2|^2 + |H_3|^2 + \cdots] + \\ & \phi_{0_1} 2Re(H_1\bar{H}_2 + H_2\bar{H}_3 + \cdots) + \\ & \phi_{0_2} 2Re(H_1\bar{H}_3 + H_2\bar{H}_4 + \cdots) + \\ & \cdots + \\ & \phi_{0_m} 2Re(H_1\bar{H}_m + H_2\bar{H}_{m+1} + \cdots)\end{aligned}$$

where H_n is the frequency response function found for the nth segment, ϕ_0 is the spectrum for $\xi = 0$ [the same as Eq. (8)], ϕ_{0m} is the cross spectrum associated with a separation distance of $\xi = s/L = m\varepsilon/L$, where ε is the segment length, and where Re denotes the real part. Values of A and N_0 then follow from ϕ_x just as in the case of uniform spanwise gusts, Eqs. (9) and (10).

Some mention should be made in this section of the problem of 3-dimensional gust encounter, wherein the longitudinal, lateral and vertical gusts components must be treated simultaneously. References 31 and 33 develop the essentials for treating this problem. It is shown in Ref. 33 that, generally, longitudinal gusts may be ignored, that wing loads are governed primarily by vertical gusts, and that fuselage and tail loads can be found by superimposing results that are obtained in separate treatments for vertical and lateral gust encounter.

Gust Response Control

As mentioned earlier in this paper, the gust response problem is one of the oldest and perhaps the chief forced response aeroelastic problem of large aircraft, having influence on airplane strength, structural fatigue life, pilot and passenger comfort, navigation and aiming, and target delivery. Because of the widespread effects of gust encounter, there has always been a continuing interest for devising means to alleviate or control the

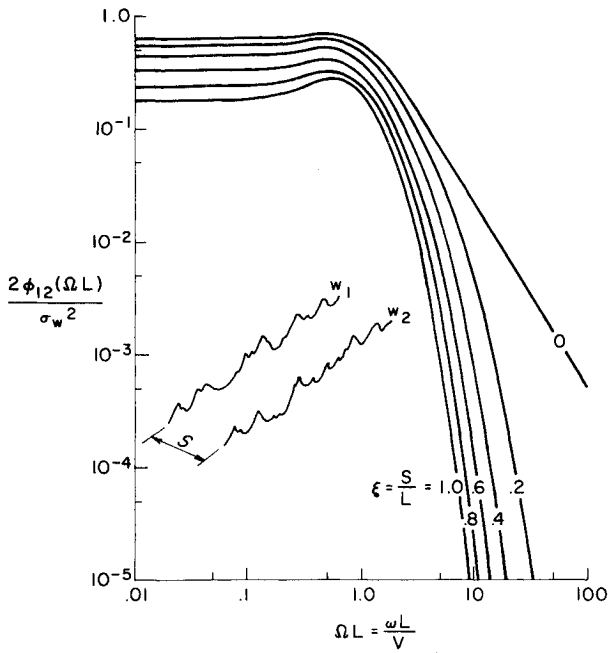

Fig. 32 Cross-spectral curves for treating nonuniform spanwise gusts.

loads and motion that result. In recent years there has been a strong resurgence of interest in the subject, and many programs of study by the manufacturers of large aircraft have been made.[34,35] A review of the subject, giving many references, is given in Ref. 36.

The main effort in the past has been attempts to alleviate loads and motion as though the airplane behaved essentially as a rigid body. Some of the more recent work also includes concepts of controlling the elastic mode response of the airframe. Terminology often used is mode stabilization or modal response control. Thus, the scope of the effort involved is much greater than it formerly was. It is noted that gust alleviation, mode stabilization, etc., may sometimes mean the same thing, but other times not. For simplicity, it would appear appropriate to use the terminology "gust response control" to include all phases of effort.

Interest in gust response control has been renewed for several reasons. The need is greater, more is known about the problem, and the subject now includes the idea of suppressing structural bending effects. With respect to these flexibility effects, much has been learned from technological developments in the launch vehicle field, where the inclusion of structural mode interaction is usually an integral part of the flight control problem. Reference 37 gives a very good summary of control system developments in the launch vehicle area. Another reason sometimes given as to why gust alleviation devices now have a better chance of becoming successful is that airplanes have become more sophisticated and versatile in their component buildup. The idea is that many of the required pieces of hardware may now exist for other reasons, or will exist in the complex future designs being considered, and that this equipment might be used to advantage for gust response control purposes without adding complexity to or compromising the design.

The basic ingredients of the gust response control problem are shown in Fig. 33. Essentially two forms of control may be involved: 1) a sensor may be used to detect the gusts, its signal being used to control some auxiliary lift device which nullifies the forces on the airplane due to the gusts, or 2) some aircraft motion may be sensed, which in turn is used to activate some control which counteracts the motion—a typical feedback loop process. These two forms may be used separately or in combination. Sensors include vanes, accelerometers, and gyros. The direct lift controls depicted are more the gust alleviation type. The force applicators provide either motion control, such as the familiar yaw dampers, or they may be used to suppress modal response. These force applicators may provide damping or stiffening action. Isolation is a possible way for some applications, but the use of this form to attenuate primary structural loads has not been developed or pursued very much to date. Geometric change is of course limited to a few configurations. Control by use of vibration-type absorbers or by increasing structural damping does not appear to be practical at the moment.

The design of gust response control systems involves consideration of a rather wide frequency spectrum; approximate ranges in frequency of various types of control systems, including the autopilot and common stability augmentation systems, are shown in Fig. 34. Additional general factors considered in the design of gust response control devices seem to be those usually associated with aircraft equipment; these include: size, weight, power consumption, complexibility and reliability, fail-safe aspects, and loop stability. In the design of gust response control systems, it is necessary to check whether loads are "alleviated" throughout the structure. A pitfall often encountered is that while a system may appear to give a load reduction in one part of the structure, it

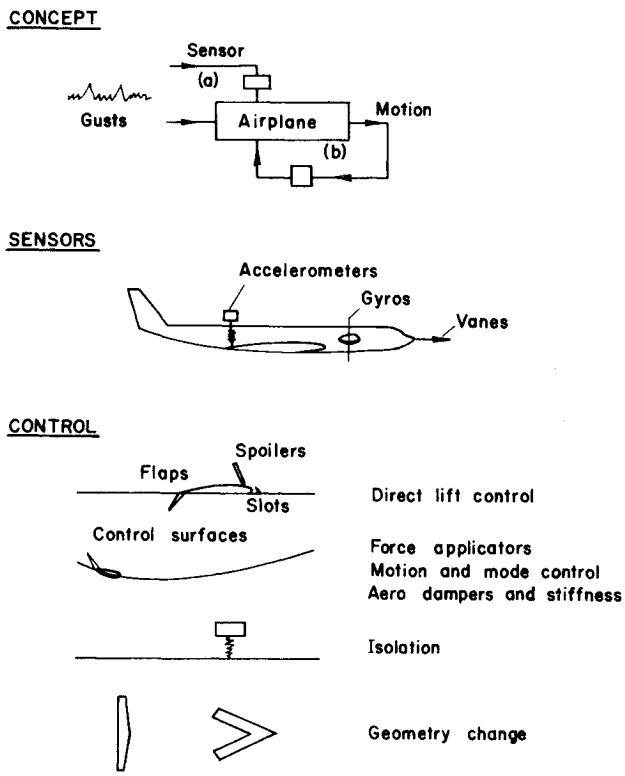

Fig. 33 Basic ingredients of load alleviation and modal suppression schemes.

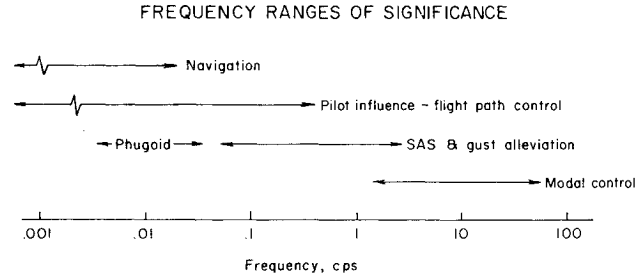

Fig. 34 Frequency ranges of concern to the aircraft engines.

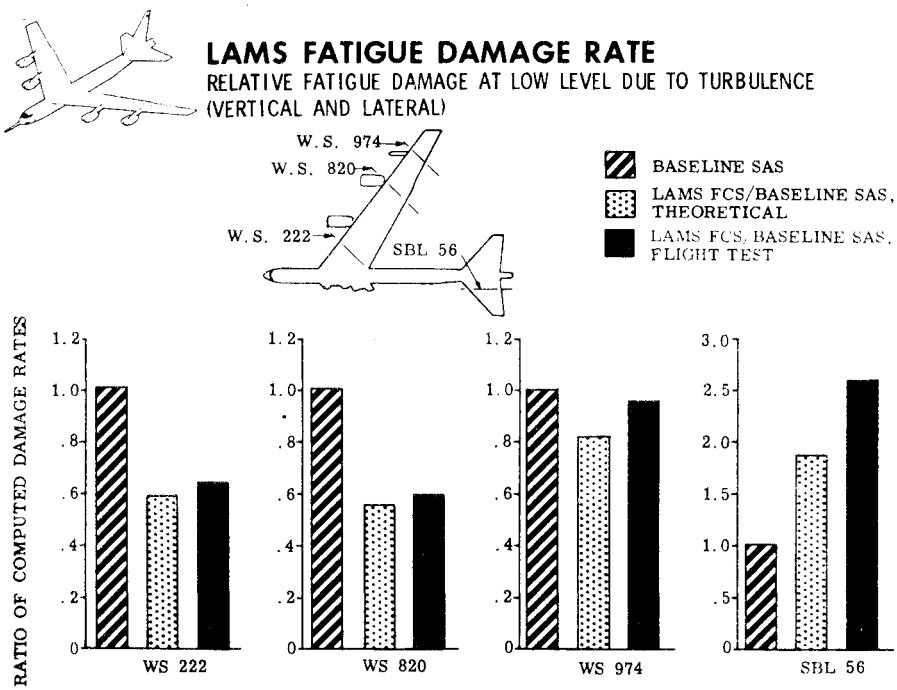

Fig. 35 Effect of modal response suppression on fatigue damage rates.

may aggravate the loads elsewhere. The system should thus do more than transfer or convert the load from one location to another; the goal in design is mainly to obtain a net over-all reduction in load and motion levels.

Figure 35 is an example of the type of results that were obtained in the LAMS (Load Alleviation and Modal Suppression) studies of the B-52 airplane.[14] Significant gains are seen to be realized in the fatigue damage rates at various wing stations; an adverse effect is noted to occur, however, in the horizontal tail.

Concluding Remarks

This paper has reviewed atmospheric turbulence and its relation to the design and flight of airplanes. An attempt has been made to give an insight to various phases of the turbulence encounter problem. Aspects considered were: the problems created by atmospheric turbulence, kinds of turbulence, mathematical modeling, turbulence measurements and airplane design and response analysis methods.

Understanding is far from complete. The detection of clear air turbulence still remains an unsolved problem. More work is needed in correlating meteorological parameters with turbulence conditions, for prediction and avoidance procedures. Turbulence parameters, such as severity, integral scale, level crossing curves, need continuing research effort so as to define design borders more reliably. More consideration must be given to 3-D turbulence encounter effects in the future. And the complicated art of gust response control must be developed along simpler and more routine lines.

References

[1] Dryden, H. L., "A Review of the Statistical Theory of Turbulence," *Turbulence*, edited by S. K. Friedlander and L. Topper, Interscience, New York, 1961, pp. 115–150.

[2] Hunsacker, J. C. and Wilson, E. B., "Report on Behavior of Aeroplanes in Gusts," Rept. 1, 1915, NACA.

[3] Report of the National Committee for Clear Air Turbulence to the Federal Coordinator for Meteorological Services and Supporting Research, U.S. Department of Commerce, Dec. 1966.

[4] Sadoff, M., Bray, R. S., and Andrews, W. H., "Summary of NASA Research on Jet Transport Control Problems in Severe Turbulence," *Journal of Aircraft*, Vol. 3, No. 3, May–June 1966, pp. 193–200.

[5] Theisen, J. G. and Haas, J., "Turbulence Upset and Other Studies on Jet Transports," *Journal of Aircraft*, Vol. 5, No. 4, July–Aug. 1968, pp. 344–353.

[6] Soderlind, P. A., "Jet Turbulence Penetration," Flight Standards Bulletin 8-63. Nov. 12, 1963, Northwest Airlines Inc., St. Paul, Minn.; also "Jet Transport Operation in Turbulence," AIAA Paper 64-353, Washington, D.C., 1964.

[7] Wolleswinkel, H. N., "Accidents in Severe Turbulence," ICAO Meeting, International Civil Aviation Organization, Montreal, Canada, Nov.–Dec. 1966.

[8] Hardy, K. R. and Ottersten, H., "Radar Investigations of Convective Patterns in the Clear Atmosphere," *Journal of Atmospheric Sciences*, Vol. 26, July 1969, pp. 666–672.

[9] Donaldson, C. duP., "A Brief Review of the Aircraft Trailing Vortex Problem," AFOSR-TR-71-1910, May 1971, Air Force Office of Scientific Research, Wright-Patterson Air Force Base, Ohio.

[10] Houbolt, J. C., "Aircraft Response to Turbulence Including Wakes," *Aircraft Wake Turbulence and Its Detection*, Plenum Press, New York, 1971.

[11] Lumley, J. L. and Panofsky, H. A., *The Structure of Atmospheric Turbulence*, edited by R. E. Marshak, Vol. XII, Interscience, New York, 1964.

[12] Houbolt, J. C., Steiner, R., and Pratt, K. G., "Dynamic Response of Airplanes to Atmospheric Turbulence, Including Flight Data on Input and Response," TR R-199, June 1964, NASA.

[13] Jones, J. W., Mielke, R. H., Jones, G. W., et al., "Low Altitude Atmospheric Turbulence, LO-LOCAT Phase III," Vol. I, Pt. I, Data Analysis, AFFDL-TR-70-10, Nov. 1970, Air Force Flight Dynamics Lab., Wright-Patterson Air Force Base, Ohio.

[14] Meeting on Aircraft Response to Turbulence, Compilation of papers presented at the NASA Langley Research Center, Sept. 24–25, 1968.

[15] Bannon, J. K., "Turbulence in the Stratosphere and in the Upper Troposphere," *Atmospheric Turbulence and Its Relation to Aircraft*, Royal Aircraft Establishment, Farnborough, England, Nov. 16, 1961, pp. 111–127.

[16] Jones, J. W., Mielke, R. H., Jones, G. W., et al., "Low Altitude Atmospheric Turbulence, LO-LOCAT Phase III," Vol. II. Pt. II. Frequency Data Plots, AFFDL-TR-70-10, Nov. 1970, Air Force Flight Dynamics Lab., Wright-Patterson Air Force Base, Ohio.

[17] Payne, F. R. and Lumley, J. L., "One-Dimensional Spectra Derived from an Airborne Hot-Wire Anemometer, *Journal of Royal Meteorological Society*, Vol. 92, No. 393, July 1966.

[18] Dempster, J. B., "Spanish Peak Gust Encounter," Sept. 1971, The Boeing Co., Wichita, Kansas.

[19] Zbrozek, J. K., "Atmospheric Gusts, Present State of the Art and

Further Research," *Journal of The Royal Aeronautical Society*, Vol. 69, No. 649, Jan. 1965.

[20] Reiter, E. R., "Clear Air Turbulence: More Problems than Solutions," Colorado State Univ., Fort Collins, Colo.

[21] Houbolt, J. C., Williamson, G. G., and Jones, B. H., "Effect of Filtering on Statistical Properties of Random Functions," AFOSR 69-3036TR, Nov. 1969, Air Force Office of Scientific Research, Wright-Patterson Air Force Base, Ohio.

[22] Bendat, J. S. and Piersol, A. G., *Random Data: Analysis and Measurement Procedures*, Wiley, New York, 1971.

[23] Houbolt, J. C., Unpublished Analysis, 1971, Aeronautical Research Associates of Princeton Inc., Princeton, N.J.

[24] Donaldson, C. duP. and Sullivan, R. D., "The Application of Invariant Modeling to the Calculation of Atmospheric Turbulence," AFFDL TR-71-168, Jan. 1972, Air Force Flight Dynamics Lab., Wright-Patterson Air Force Base, Ohio.

[25] Houbolt, J. C., "Gust Design Procedures Based on Power Spectral Techniques," AFFDL-TR-67-74, Aug. 1967, Air Force Flight Dynamics Lab., Wright-Patterson Air Force Base, Ohio.

[26] Houbolt, J. C., "Design Manual for Vertical Gusts Based on Power Spectral Techniques, AFFDL-TR-70-106, Dec. 1970, Air Force Flight Dynamics Lab., Wright-Patterson Air Force Base, Ohio.

[27] Houbolt, J. C., "The Art of Determining Gust Frequency Response Functions," presented at the 31st AGARD Structures and Materials Panel Meeting, Tønsberg, Norway, Oct.-Nov. 1970.

[28] Hoblit, F. M., Paul, N., Shelton, J. D., and Ashford, F. E., "Development of a Power-Spectral Gust Design Procedure for Civil Aircraft," FAA-ADS-53, Jan. 1966, Federal Aviation Agency.

[29] Houbolt, J. C., "On the Response of Structures Having Multiple Random Inputs," *Jahrbuch 1957 der Wissenschaftlichen Gesellschaft für Luftfahrt E.V. (WGL)*, Vieweg & Sohn, Braunschweig, pp. 296–305.

[30] Diederich, F. W., "The Response of an Airplane to Random Atmospheric Disturbances," Rept. 1345, 1958, NACA; Supersedes TN 3910, NACA.

[31] Eichenbaum, F. D., "A General Theory of Aircraft Response to Three-Dimensional Turbulence," *Journal of Aircraft*, Vol. 8, No. 5, May 1971, pp. 353–360.

[32] Houbolt, J. C. and Sen, A., "Cross-Spectral Functions Based on von Kármán's Spectral Equation," CR-2011, March 1972, NASA.

[33] Houbolt, J. C., "On the Response of Airplanes in a 3-Dimensional Gust Field," Rept. 161, July 1971, Aeronautical Research Associates of Princeton Inc., Princeton, N.J.

[34] Wykes, J. J. and Mori, A. S., "An Analysis of Flexible Aircraft Structural Mode Control," Pt. 1, AFFDL-TR-65-190, June 1966, Air Force Flight Dynamics Lab., Wright-Patterson Air Force Base, Ohio.

[35] Burris, P. M. and Bender, M. A., "Aircraft Load Alleviation and Mode Stabilization (LAMS), B-52 System Analysis, Synthesis, and Design," AFFDL-TR-68-161, Nov. 1969, Air Force Flight Dynamics Lab., Wright-Patterson Air Force Base, Ohio.

[36] Davis, H. Max and Swaim, Dr. R. L., "Control of Flexible Aircraft Dynamic Response," presented at the AGARD Specialists Meeting on Stability and Control, Sept. 20–23, 1966, Cambridge, England.

[37] Blair, J. C., Lovingood, J. A., and Geissler, E. D., "Advanced Control Systems for Launch Vehicles," *Astronautics and Aeronautics*, Aug. 1966, p. 30.